Journal of
Experimental
Botany
www.jxb.oxfordjournals.org

RESEARCH PAPER

Differentiation of C₄ photosynthesis along a leaf developmental gradient in two *Cleome* species having different forms of Kranz anatomy

Nuria K. Koteyeva[1], Elena V. Voznesenskaya[1], Asaph B. Cousins[2] and Gerald E. Edwards[2,*]

[1] Laboratory of Anatomy and Morphology, V. L. Komarov Botanical Institute of Russian Academy of Sciences, Prof. Popov Street 2, 197376, St. Petersburg, Russia
[2] School of Biological Sciences, Washington State University, Pullman, WA 99164-4236 USA

* To whom correspondence should be addressed. E-mail: edwardsg@wsu.edu

Abstract

In family Cleomaceae there are NAD-malic enzyme-type C₄ species having different forms of leaf anatomy. Leaves of *Cleome angustifolia* have Glossocardioid-type anatomy with a single complex Kranz unit which surrounds all the veins, while *C. gynandra* has Atriplicoid anatomy with multiple Kranz units, each surrounding an individual vein. Biochemical and ultrastructural differentiation of mesophyll (M) and bundle sheath (BS) cells were studied along a developmental gradient, from the leaf base (youngest) to the tip (mature). Initially, there is cell-specific expression of certain photosynthetic enzymes, which subsequently increase along with structural differentiation. At the base of the leaf, following division of ground tissue to form M and BS cells which are structurally similar, there is selective localization of Rubisco and glycine decarboxylase to BS cells. Thus, a biochemical C₃ default stage, with Rubisco expression in both cell types, does not occur. Additionally, phosphoenolpyruvate carboxylase (PEPC) is selectively expressed in M cells near the base. Surprisingly, in both species, an additional layer of spongy M cells on the abaxial side of the leaf has the same differentiation with PEPC, even though it is not in contact with BS cells. During development along the longitudinal gradient there is structural differentiation of the cells, chloroplasts, and mitochondria, resulting in complete formation of Kranz anatomy. In both species, development of the C₄ system occurs similarly, irrespective of having very different types of Kranz anatomy, different ontogenetic origins of BS and M, and independent evolutionary origins of C₄ photosynthesis.

Key words: C₄ anatomy, C₄ development, *Cleome angustifolia*, *Cleome gynandra*, C₄ photosynthesis, C₄ plants, immunolocalization, ultrastructure.

Introduction

In most C₄ plants, the dual-cell system (so-called Kranz anatomy) operates to concentrate CO₂ around ribulose 1,5-bisphosphate carboxylase-oxygenase (Rubisco). Primary fixation of CO₂ into C₄ acids occurs in the outer layer of mesophyll (M) cells using phosphoenolpyruvate carboxylase (PEPC), while decarboxylation of C₄ acids and refixation of CO₂ by Rubisco in the C₃ pathway occur in the inner layer of bundle sheath (BS) cells (Hatch, 1987). This CO₂-concentrating mechanism restricts the competing ribulose bisphosphate (RuBP) oxygenase reaction and synthesis of glycolate, and the loss of CO₂ by photorespiration. Glycine decarboxylase (GDC), which is essential for photorespiratory

CO_2 release in the glycolate pathway, is confined exclusively to BS mitochondria (Edwards and Walker, 1983; Edwards and Voznesenskaya, 2011; Sage *et al.*, 2012).

C_4 species are classified according to their biochemical subtype based on the predominant type of C_4 decarboxylase, NADP-malic enzyme (NADP-ME), NAD-malic enzyme (NAD-ME), or phosphoenolpyruvate carboxykinase, used to release and concentrate CO_2 around Rubisco (Hatch, 1987). The two main types of C_4 cycles in eudicots function either through NADP-ME, which is located in the chloroplasts, or through NAD-ME, which is located in the mitochondria of BS cells. There are structural differences in grana development between M and BS chloroplasts in NADP-ME- versus NAD-ME-type C_4 species associated with differences in photochemistry. For C_4 to function, NADPH is required to reduce 3-phosphoglycerate, the product of CO_2 fixation by Rubisco, to triose-phosphates. In NADP-ME-type C_4 species, the primary shuttle of malate from M cells to BS chloroplasts provides both CO_2 and NADPH, which reduces the requirement for photosystem II (PSII) activity, and the associated development of grana, in BS chloroplasts. In NAD-ME-type species, BS chloroplasts have increased grana development and PSII activity, since the primary shuttle of aspartate from the M to BS cells delivers CO_2, but not reductive power (Edwards and Walker, 1983; Edwards and Voznesenskaya, 2011).

C_4 photosynthesis is considered to have evolved independently >60 times (Sage *et al.*, 2011), resulting in much structural diversity in the forms of C_4 which evolved from C_3 ancestors (Dengler and Nelson, 1999; Peter and Katinas, 2003; Muhaidat *et al.*, 2007; Edwards and Voznesenskaya, 2011). Among the forms identified, 16 develop Kranz around individual veins, while eight develop a compound Kranz unit near the periphery of the leaf, which surrounds all veins (Edwards and Voznesenskaya, 2011). The diversity in forms occurs by special positioning of the M and BS layers in relation to the distribution of veins and other tissues, by the occurrence of different types of tissues in the leaf (e.g. mestome sheath in monocots, hypodermal, or water storage cells in dicots), by the way organelles (chloroplast and mitochondria) are arranged in BS cells and their differentiation between M and BS cells, and by structural diversity in developing gas diffusion barriers to support the CO_2-concentrating mechanism (Edwards and Voznesenskaya, 2011).

The ontogeny of the complex C_4 system requires a highly coordinated selective expression of many genes during development, concurrent with establishment of Kranz anatomy. Genes controlling development of M and BS specialization for function of the C_4 system, and the degree of redundancy which has occurred during the multiple times C_4 has evolved is unknown. Among monocot and eudicot C_4 species which are being used as genetic models, concerted efforts are needed to identify regulatory factors along leaf developmental gradients which control the expression of specific C_4 traits (Covshoff *et al.*, 2013).

There have been a number of studies on structural and biochemical development of forms of C_4 having Kranz anatomy around individual veins. This includes extensive analysis of leaf development in *Zea mays* which has classical NADP-ME-type anatomy (Sheen and Bogorad, 1985; Langdale *et al.*, 1988b; Dengler and Nelson, 1999; Sheen, 1999). In the interest of identifying transcription factors controlling expression of specific traits which are required for C_4 function, there have been recent studies on the developmental gradient along the leaf of maize, including analyses of transcriptome, proteome, and structural changes (see Li *et al.*, 2010; Majeran *et al.*, 2010; Covshoff *et al.*, 2013; Wang *et al.*, 2013). Developmental studies have also been conducted on some other forms of Kranz anatomy in grasses (Dengler *et al.*, 1985, 1986, 1996; Wakayama *et al.*, 2003) and on different structural forms of Kranz in family Cyperaceae (Soros and Dengler, 2001). Among eudicots, significant developmental studies have been conducted on two NAD-ME-type species having Atriplicoid-type anatomy, namely *Atriplex rosea* (Liu and Dengler, 1994; Dengler *et al.*, 1995; Dengler and Nelson, 1999) and *Amaranthus hypochondriacus* (Ramsperger *et al.*, 1996; Patel and Berry, 2008). There has been less attention to development of types of Kranz anatomy which surround all veins in the leaves. There are reports on NADP-ME Salsoloid type with *Salsola richteri* (Voznesenskaya *et al.*, 2003b), NAD-ME Salsinoid type with *Suaeda taxifolia*, and NAD-ME Schoberioid type with *Suaeda eltonica* (Koteyeva *et al.*, 2011a).

These studies on different forms of C_4 show a progression in structural and biochemical differentiation during development, with dimorphic M and BS cells originating from monomorphic cells. Characterization of the development of Kranz anatomy includes identification of the origins of M and BS cells during leaf initiation, which is different depending on Kranz anatomical type or plant lineages (Dengler *et al.*, 1985; Dengler and Nelson, 1999; Soros and Dengler, 2001; Koteyeva *et al.*, 2011a). This characterization includes structural differentiation of M and BS chloroplasts and their function in photochemistry to provide energy cooperatively for CO_2 assimilation (Brown, 1975; Dengler *et al.*, 1985; Langdale *et al.*, 1988a, b; Dengler and Nelson, 1999; Sheen, 1999; von Caemmerer and Furbank, 2003; Patel and Berry, 2008; Li *et al.*, 2010; Majeran *et al.*, 2010; Edwards and Voznesenskaya, 2011; Koteyeva *et al.*, 2011a; Wang *et al.*, 2013). It also consists of analysis of the differences among forms of C_4 in the development of barriers to diffusion of CO_2 from sites of decarboxylation in BS cells, which enables CO_2 to be concentrated around Rubisco (e.g. BS cell wall thickness, location of the C_4 acid decarboxylase, and the position of organelles) (von Caemmerer and Furbank, 2003). Determining when selective expression of enzymes in M and BS cells for C_4 function occurs during development among different forms of C_4 is also important (Dengler *et al.*, 1985; Soros and Dengler, 2001; Koteyeva *et al.*, 2011a; Langdale, 2012). Analyses show that there are differences in the sequence and the timing of biochemical and structural changes, with respect to establishment of the vascular system, and whether expression of traits is regulated by environmental (light) or developmental cues (Langdale *et al.*, 1988a; Wang *et al.*, 1992; Dengler *et al.*, 1995; Ramsperger *et al.*, 1996; Dengler and Nelson, 1999; Sheen, 1999; Voznesenskaya

et al., 2003a; Wakayama *et al.*, 2003; Koteyeva *et al.*, 2011a; Langdale, 2012).

There is recent interest in the occurrence of C$_4$ photosynthesis in Cleomaceae, one of 19 families in which C$_4$ species have been found (Sage *et al.*, 2011). The genus *Cleome sensu lato* consists of >200 species. Most species have the C$_3$ type of photosynthesis; but, it has been shown that three species, *Cleome angustifolia*, *C. gynandra*, and *C. oxalidea*, have NAD-ME-type C$_4$ photosynthesis in leaves and cotyledons (Marshall *et al.*, 2007; Voznesenskaya *et al.*, 2007; Feodorova *et al.*, 2010; Koteyeva *et al.*, 2011b). Two of them, *C. gynandra* and *C. oxalidea*, have flat leaves with an Atriplicoid type of anatomy consisting of multiple Kranz units around individual veins, while *C. angustifolia* with Glossocardioid-type anatomy, has a single compound Kranz unit with a double layer of concentric chlorenchyma surrounding all the veins and water storage cells (Koteyeva *et al.*, 2011b). They belong to separate lineages in the genus and they have different distribution, pantropical for *C. gynandra*, Australian for *C. oxalidea*, and African for *C. angustifolia* (Feodorova *et al.*, 2010). *Cleome gynandra* was originally proposed as a model NAD-ME eudicot C$_4$ species for identifying factors controlling development and function of C$_4$ photosynthesis (Brown *et al.*, 2005). The attractive features of this species are that it can be transformed, grown under a short life cycle, has C$_3$ and C$_3$–C$_4$ intermediate *Cleome* relatives for comparative studies, and, phylogenetically, among C$_4$ genera it has the closest position to the well-established model species *Arabidopsis thaliana* (a C$_3$ dicot) (Feodorova *et al.*, 2010; Covshoff *et al.*, 2013). Progress towards development of *C. gynandra* has been made, including identifying transcripts associated with C$_4$ biochemistry and metabolite transporters (Kajala *et al.*, 2012), in comparative RNaseq profiling (Bräutigam *et al.*, 2011), and in the ability to transform it (Newell *et al.*, 2010).

The purpose of the current study was to examine development of C$_4$ in two NAD-ME-type C$_4$ *Cleome* species, *C. gynandra* and *C. angustifolia*, which have major differences in leaf morphology, vascular pattern, and forms of Kranz anatomy. This included analysis of M and BS cell formation from leaf primordia, and structural and biochemical transitions during leaf ontogeny, to determine whether there is convergence in development and expression of C$_4$ traits.

Materials and methods

Plant material

Seeds of *Cleome angustifolia* Forssk. (from herbarium material kindly provided by Drs A. Oskolskii and O. Maurin) and *C. gynandra* L. (kindly provided by Dr A.S. Raghavendra) were stored at 3–5 °C prior to use and were germinated on moist paper in Petri dishes at room temperature and a photosynthetic photon flux density ~20 μmol quanta m^{-2} s^{-1}. The seedlings were then transplanted to 15 cm diameter pots with commercial potting soil and grown in the greenhouse during the mid-winter/spring months, with an approximate 26 °C day/18 °C night temperatures. Maximum midday photosynthetic photon flux density was 500 μmol quanta m^{-2} s^{-1} on clear days. Plants were fertilized once a week with Peter's Professional (20:20:20; Scotts Miracle-Gro Co., Marysville, OH, USA). For microscopy and biochemical analyses, leaves of different

lengths were taken from plants of ~3–6 weeks old. Voucher specimens are available at the Marion Ownbey Herbarium, Washington State University under # WS 375818 for *C. angustifolia* and WS 369765 for *C. gynandra.*

Light and electron microscopy

Study of the structural basis of leaf development was carried out on expanding leaves with lengths of leaflets from 0.5 mm to 7 mm. Vegetative shoot tips were used to study the earliest events of leaf initiation and development. Three samples of each leaflet length (using the terminal leaflet in the palmate leaf) were harvested from three independent plants of each species (a total of nine samples from each species for each leaf length). Vegetative shoot apices with several of the youngest leaf primordia, and leaves of intermediate size (6–7 mm in length), were sectioned longitudinally. Additionally, cross-sections were made in 0.5 mm steps from the tip to base of 3–5 mm long leaves.

Sample preparation for light microscopy (LM) and transmission electron microscopy (TEM) was carried out following Koteyeva *et al.* (2011a). An Olympus BH-2 (Olympus Optical Co. Ltd) light microscope equipped with an LM Digital Camera and Software (Jenoptik ProgRes Camera, C12plus, Jena, Germany) was used for observation and collection of images at the LM level. A Hitachi H-600 (Hitachi Scientific Instruments, Tokyo, Japan) and FEI Tecnai G2 (Field Emission Instruments Company, Hillsboro, OR, USA) equipped with Eagle FP 5271/82 4K HR200KV digital camera transmission electron microscopes were used for TEM studies.

The cell size, length of the chloroplasts, and the thickness of cell walls were measured for the adaxial M and BS on micrographs from leaf longitudinal and cross-sections at different distances from the leaf base using an image analysis program (UTHSCSA, Image Tool for Windows, version 3.00). For both types of cells, the measurements of cell wall thickness were made on cell walls facing intercellular airspaces between M and BS. From images of the cell walls, plasmodesmata between M and BS cells (which were radially but not longitudinally oriented in the wall sections) were counted. The plasmodesmata frequency was referred to as the number of plasmodesmata per 1 μm of cell–cell contact interface length.

Images of the shoot apices with the youngest leaf primordia and surface of young leaves for analysis of stomata were captured under the low vacuum mode with an FEI Scanning Electron Microscope Quanta 200F (Feild Emission Instruments Company) without additional treatments.

To observe the leaf vascular pattern, leaves of different ages, from youngest primordia to fully expanded leaves, were cleared in 70% ethanol (v/v) until chlorophyll was removed, bleached with 5% (w/v) NaOH overnight, and then rinsed three times in water. At least five leaves of different ages were studied from two to three different plants. The leaves were mounted in water on slides and examined under a UV light [with a 4′,6-diamidino-2-phenylindole (DAPI) filter] on a Fluorescence Microscope Leica DMFSA (Leica Microsystems Wetzlar GmbH, Germany) using autofluorescence of lignified tracheary elements of the xylem.

In situ *immunolocalization*

Sample preparation and immunolocalization by LM and TEM were carried out on longitudinal sections of leaves, 6–7 mm long, following the procedure in Koteyeva *et al.* (2011a). Antibodies used were anti-spinach Rubisco [large subunit (LSU)] IgG (courtesy of B. McFadden) commercially available anti-maize PEPC IgG (Chemicon, Temecula, CA, USA), and the P-subunit of GDC, all raised in rabbits. The density of labelling was determined by counting the gold particles on digital electron micrographs using the UTHSCSA image analysis program and calculating the number per unit area (μm^2). Standard errors were determined.

Western blot analysis

For the study of accumulation of the main photosynthetic enzymes during development, individual leaflets of different ages, with lengths of 1–3, 3–6, 6–10, 10–15 mm, and 30–35 mm (totally expanded mature leaflet), were used. Soluble proteins were extracted from leaves and prepared for SDS–PAGE following Koteyeva *et al.* (2011b). Protein concentration was determined with an RCDC protein quantification kit (Bio-Rad), which tolerates detergents and reducing agents. A 10 µg aliquot of soluble protein was applied per lane, with separation by 12% (w/v) SDS–PAGE, and transferred to a nitrocellulose membrane for analysis of the several photosynthetic enzymes and GDC. Primary antibodies used were anti-*Amaranthus hypochondriacus* NAD-ME IgG against the 65 kDa α-subunit (Long and Berry, 1996) (dilution 1:5000), anti-*Zea mays* PEPC IgG (1:100 000), anti-*Zea mays* pyruvate,Pi dikinase (PPDK) IgG (courtesy of T. Sugiyama) (1:5000), anti-*Pisum sativum* L. GDC P-subunit (courtesy of Dr D. Oliver) (1:10 000), and anti-*Spinacia oleracea* Rubisco LSU IgG (courtesy of B. McFadden) (1:10 000). Goat anti-rabbit IgG–alkaline phosphatase-conjugated secondary antibodies (Sigma) were used at a dilution of 1:10 000 for detection. Bound antibodies were visualized by developing the blots with 20 mM nitroblue tetrazolium and 75 mM 5-bromo-4-chloro-3-indolyl phosphate in detection buffer (100 mM TRIS-HCl, pH 9.5, 100 mM NaCl, and 5 mM $MgCl_2$). Two separate blots from two separate extractions were made for each enzyme. The intensities of bands in western blots were quantified with an image analysis program (ImageJ 1.37, NIH, USA) and expressed relative to the level in the fully expanded leaves.

Mass spectrometric measurements of Γ, R_d, and leaf carbon isotope composition

A membrane inlet mass spectrometer (DELTA V Plus; Thermo Scientific) connected to a closed leaf chamber via a membrane inlet was used to measure rates of CO_2 exchange and the CO_2 compensation point (Γ) in *C. gynandra* young and mature leaves, as described previously (Maxwell *et al.*, 1998; Ruuska *et al.*, 2000). Cuttings from mature leaves ~1.5 cm^2 or 5–7 young (~7 mm) leaves of *C. gynandra* harvested from several branches were placed in the chamber and, once CO_2 and O_2 concentrations were balanced with ambient concentrations, the leaf chamber was sealed and after 5 min sitting in the dark was submitted to an irradiance of 1000 µmol m^{-2} s^{-1}. The temperature was controlled at 25 °C using a water bath circulating around the chamber. Net CO_2 assimilation was followed in the sealed chamber by measuring the changes in $^{12}CO_2$ concentration over time until reaching Γ; that is, when the amount of CO_2 assimilated by photosynthesis was balanced with the amount of CO_2 released by respiration and photorespiration. The rate of dark respiration (R_d) was calculated from the rate of CO_2 released after a minimum of 5 min in the dark. The system was zeroed before and after each measurement by flushing the chamber with a mixture of nitrogen and oxygen.

Leaf carbon isotope composition was determined in *C. gynandra* from sections taken at the base, middle, and tip of young 0.7 cm leaves, and from mature leaves (n=3–6). As previously described (Voznesenskaya *et al.*, 2013), samples (1–2 mg) were placed in a tin capsule and combusted in a Eurovector elemental analyser; the resulting N_2 and CO_2 gases were separated by gas chromatography and admitted into the inlet of a Micromass, Isoprime isotope ratio mass spectrometer (IRMS) for determination of $^{13}C/^{12}C$ ratios (R). δ^{13}C values were determined where $1000 \times R_{sample}/R_{standard})-1$, using PDB (Pee Dee Belemnite) as the standard.

Statistical analysis

Where indicated, standard errors were determined, and analysis of variance (ANOVA) was performed with Statistica 7.0 software (StatSoft, Inc.). Tukey's HSD (honest significant difference) tests were used to analyse differences in cell and chloroplast sizes, cell wall thickness, plasmodesmata frequency, amounts of gold particles, intensities of bands in western blots, and Γ and R_d values at different stages of leaf development. All analyses were performed at the 95% significance level.

Results

Early events in primary leaf morphogenesis

Cleome angustifolia and *C. gynandra* have palmate compound leaves with up to five flat, broad leaflets in *C. gynandra* and 5–8 narrow leaflets in *C. angustifolia*. Figure 1 shows the morphology and anatomy of a vegetative shoot apical meristem of *C. angustifolia* and *C. gynandra* at the stage of active organogenesis, together with the early stages of morphogenesis of compound leaves (Fig. 1A–D). Leaf primordia in both species are initiated alternately. When the primordium reaches ~100 µm, the proliferation of marginal and submarginal initials appears at the distal adaxial flank (Fig. 1B), giving rise to the terminal followed by the lateral primordial leaflets (Fig. 1A, C). Leaflets of *C. angustifolia* grow by meristem initials at the base generating files of cells with restricted marginal growth resulting in narrow leaflets. Laminar growth in the leaflets of *C. gynandra* is initiated when they reach 0.4–0.5 mm long, forming a flat blade (Fig. 1D).

In both species, the processes of tissue differentiation in terminal and lateral leaflets are similar; but they differ in growth dynamics, resulting in different sizes (Fig. 1A, C). Procambial strands of the future major veins are initiated acropetally (developing from the base towards the tip) in leaflets. From analysis of cleared young leaves of different ages, the visualization of lignified elements of xylem confirms an acropetal pattern of differentiation of major veins, and shows a basipetal pattern of peripheral/minor vasculature development. In *C. angustifolia*, the lateral veins develop from the tip (Fig. 1E). In general, *C. gynandra* also has a basipetal pattern of secondary vascular system development from the tip of the leaf and the leaf margins to the base; however, veins of different orders have different time courses of initiation, with later development of the higher order veins (not shown).

Leaflet development in compound leaves does not differ from that in simple leaves, as shown earlier for different species (Esau, 1965). The leaflet of *Cleome* species will be referred to later as 'leaf' for simplicity in presentation.

Ontogenetic origin of mesophyll and bundle sheath cells

The origin of M and BS cells was observed in cross- and longitudinal sections at the base of young leaves (leaf length of 0.5–5 mm for *C. angustifolia* and 3–7 mm for *C. gynandra*). In *C. angustifolia*, M and BS cell precursors originate during the initiation of leaf primordium from the ground meristem, with subsequent division of abaxial M progenitors which give rise to the M layer adjacent to BS cells and an additional layer of abaxial chlorenchyma [precursors of the spongy mesophyll (SM) cell layer]. The middle layers of ground meristem generate water storage tissue and procambial strands. Young
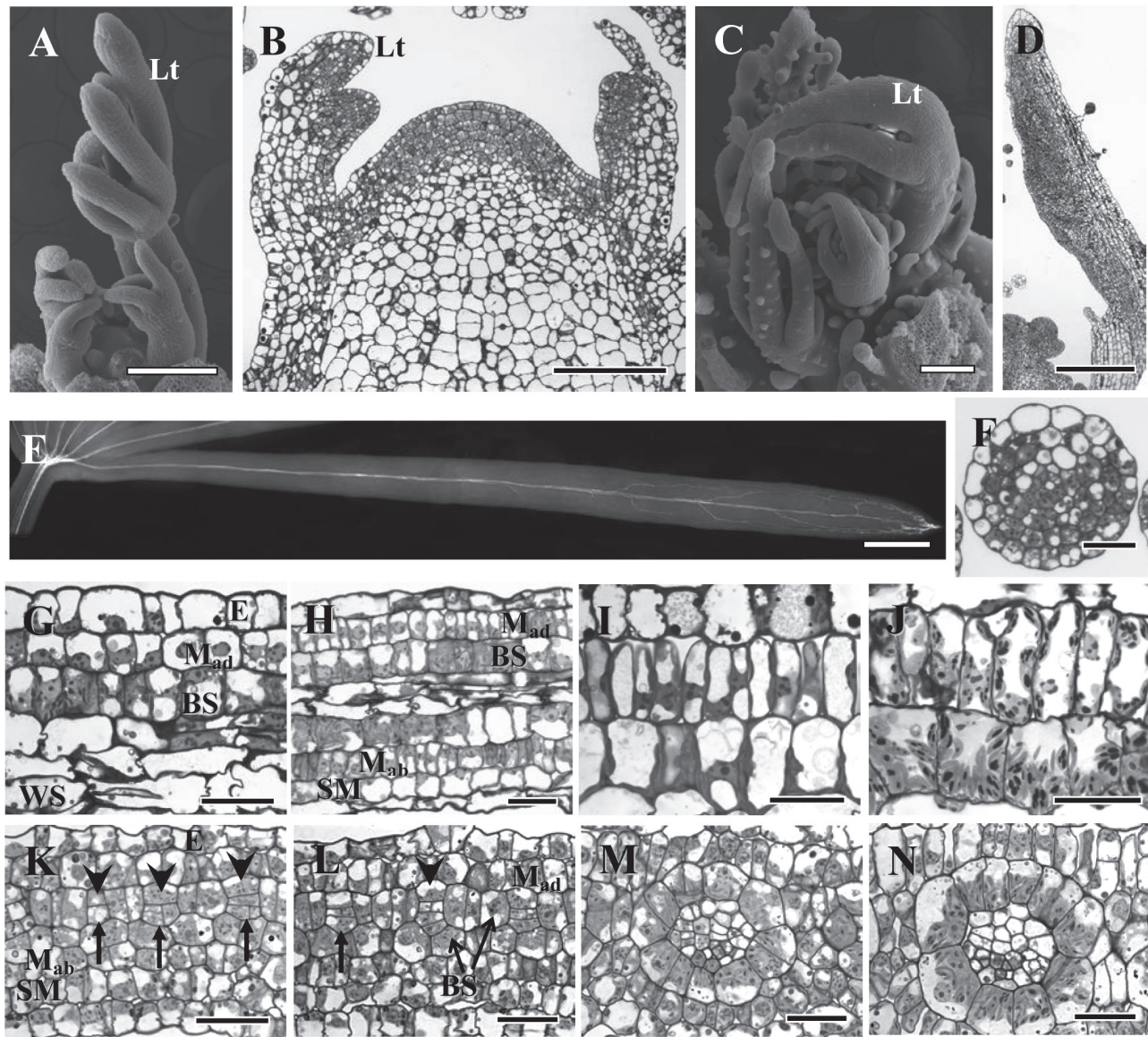
Fig. 1. Vegetative shoot tip structure and early stages of leaf development in two *Cleome* species, *C. angustifolia* (A, B, E–J) and *C. gynandra* (C, D, K–N). (A, C) Scanning electron microscopy of shoot tips. (B, D) Light microscopy of longitudinal sections of the shoot apical meristem showing initiation and development of the leaflet. (E) Cleared young leaflet of *C. angustifolia* under UV light showing the basipetal direction of lateral vein development. (F) Cross-section of the young (0.5 mm) *C. angustifolia* leaf. (G–J) Longitudinal sections showing the formation of cell lineages from the base of young leaves (G) to the tip (J), with the direction of maturation from left to right in *C. angustifolia*. The adaxial double-layered chlorenchyma (M and BS) differentiation is shown at Stages 1 (G), 2 (H, note the abaxial SM delimited), 3 (I), and 4 (J). (K–N) Procambial strand initiation and Kranz anatomy development around the veins from the base of young leaves (K) to the tip (N), with the direction of maturation from left to right in *C. gynandra*. (K) Procambium initials are indicated by arrows; arrowheads show the first adaxial BS cell progenitor; note the additional abaxial SM layer formed. (L) BS progenitors derived from second and third ground meristem layers are indicated. Different stages of M and BS differentiation are shown for *C. gynandra*: Stage 1 (L), 2 (M), and 3 (N). E, epidermis; BS, bundle sheath; Lt, leaflet; M_{ad}, adaxial mesophyll; M_{ab}, abaxial mesophyll; SM, spongy mesophyll; WS, water storage. Scale bars=200 µm for A, C, D; 100 µm for B; 0.5 mm for E; 20 µm for F–N.

leaf primordia (up to 0.5 mm) consist of 6–7 layers of ground meristem and the forming central procambial strand (excluding epidermis, Fig. 1F). During the subsequent leaf blade development, the M and BS cells divide only anticlinally, and the developing leaf consists of 7–8 cell layers between epidermises depending on the number of progenitors of water storage cells (Fig. 1H).

In *C. gynandra*, the youngest leaves (up to 3 mm long) and the base of young leaves (7 mm long) consist of four layers of ground meristem between the adaxial and abaxial epidermis (not shown), with the abaxial subepidermal cells undergoing periclinal divisions very early in development and forming an additional abaxial layer which will later become SM (Fig. 1K, L). Periclinal division of the ground meristem cells in the second layer leads to initiation of the procambial strand from the abaxial derivative (Fig. 1K, arrows show the different stages of procambial strand formation). The adaxial derivative is the progenitor of the upper BS cell (or 2–4 upper BS cells in the case of subsequent anticlinal divisions; Fig. 1K, arrowheads show the upper BS progenitors). All other BS cells originate from the second and third layers of ground meristem which surround the forming vascular tissues (Fig. 1L). The M is

differentiated from the first, second, third, or fourth layer of the ground meristem cells depending on the position of M cells around the ring (on the cross-section) of BS cells.

Development of Kranz anatomy

The formation of Kranz anatomy was studied at the LM and TEM levels using longitudinal sections of intermediate size young leaves. Clear gradual progression in distinct developmental events can be observed along the leaf from the base to the tip. In both species, the meristematic activity is evident near the base of the leaf, followed by BS cell expansion with M cell intensive divisions, resulting in 2–3 M cells per BS cell as viewed on the leaf section. In both species the additional abaxial layer of SM cells has not undergone anticlinal divisions, in contrast to their sister abaxial M (M_{ab}) cells which are adjacent to the BS (Fig. 1H, L). After transition of M cells to expansion, the structural differentiation of M and BS cells begins, and close to the leaf tip complete Kranz anatomy is established. Following the initial formation of M and BS cells from progenitor cells, four stages of chlorenchyma development were characterized in the progression towards the formation of the Kranz syndrome.

Stages of chlorenchyma development in C. angustifolia

Development was visualized using files of cells which were continuous from the base to the tip of the 6 mm long leaf. In Stage 1 at the meristematic zone of the base of the leaf (0–1 mm from the base), M and BS cells are similar in shape, size, and structure (Fig. 1G; Table 1). They can be identified by their position, from the adaxial side of the leaf subepidermal layer for M, and BS for the next layer, with an additional subepidermal layer of SM cells on the abaxial side. At this time M and BS cells undergo anticlinal divisions.

Following the completion of division of M cells, the expansion of M and BS cells is evident (~2–3 mm from the base)

(Table 1), and this was designated as Stage 2. At this time M and BS cells have a central vacuole, and chloroplasts are distributed around the cell periphery. In M cells, the nucleus often has a central position (Fig. 2A). Chloroplasts have a relatively well-developed thylakoid system with numerous small grana which are structurally similar in both M and BS cells (Fig. 2D, E). Mitochondria in the chlorenchyma cells are few in number, small, and they have crescent-like cristae (Fig. 2J). The cells of all tissues are tightly packed; minor intercellular air spaces (IAS) exist between M and epidermal cells (Fig. 2A). Xylem and phloem elements are not differentiated in veins.

Stage 3 (~3–5.5 mm from the base) of chlorenchyma development is characterized by structural differentiation of M and BS. M cells have developed a palisade shape with a well-developed central vacuole and organelles distributed around the cell periphery (Figs 1I, 2B). The characteristic centripetal positioning of organelles in BS cells is established (Fig. 1I, Fig. 2B). BS and M chloroplasts are structurally similar; but, compared with Stage 2, they have become enlarged (Table 1) and have a more developed thylakoid system (Fig. 2F, G). BS mitochondria are co-localized with chloroplasts, and they are also slightly enlarged (Fig. 2K). Intercellular air spaces throughout the M cell layer are more prominent (Figs 1I, 2B). The numbers of plasmodesmata connecting M and BS cells have increased (Fig. 2M; Table 1). At this stage, there are the first signs of vascular tissue differentiation in the minor veins. In most vascular bundles, 1–2 tracheary elements are well developed, while the sieve elements of the phloem are still not completely differentiated as they contain a cytoplasmic layer with organelles delimited by the tonoplast. Mature xylem vessels can be identified by the prominent secondary wall thickening and the lack of cytoplasm. Mature sieve tubes contain only a peripheral layer of cytosol without nuclei, ribosomes, and tonoplasts, with rare occurrence of mitochondria, plastids, and smooth endoplasmic reticulum (not shown).

Table 1. *Cell size (length, L, and width, W), thickness of cell walls, size of chloroplasts for mesophyll (M) and bundle sheath (BS) cells, and the number of plasmodesmata in the cell wall between M and BS cells*

Stage of development	Cell size (µm)				Thickness of individual cell wall towards the IAS (µm)		No. of plasmodesmata per µm M/BS cell wall	Chloroplast length (µm)	
	M		BS		M	BS		M	BS
	L	W	L	W					
Cleome angustifolia									
1	12.5±0.5 a	9.1±0.5 b	12.5±0.3 a	9.7±0.7 a	ND	ND	ND	1.5±0.07 a	1.6±0.06 a
2	15.4±0.2 b	5.4±0.3 a	16.4±0.4 b	11.1±0.6 a	0.12±0.009 a	0.23±0.01 a	0.53±0.12 a	1.5±0.08 a	2.3±0.1 a
3	20.3±0.2 c	4.9±0.2 a	19.6±0.5 b	13.1±0.4 b	0.12±0.02 a	0.27±0.01 b	1.25±0.16 b	2.3±0.08 b	3.0±0.08 b
4	35.6±1.0 d	8.5±0.4 b	27.1±0.7 c	15.6±1.1 c	0.14±0.006 a	0.28±0.01 b	1.1±0.14 b	5.6±0.2 c	4.8±0.2 c
Cleome gynandra									
1	10.3±0.3 a	6.6±0.3 a	9.7±0.3 a	10.8±0.6 a	ND	ND	ND	2.5±0.1 a	2.4±0.1 a
2	16.0±0.6 b	6.7±0.3 a	13.6±0.5 b	15.3±0.9 b	0.08±0.01 a	0.21±0.02 a	1.11±0.09 a	3.5±0.2 a	3.8±0.2 b
3	19.1±0.6 c	6.4±0.2 a	15.7±0.5 b	15.1±1.0 b	0.10±0.01 a	0.30±0.02 b	0.88±0.17 a	4.6±0.1 b	5.1±0.2 c
4	21.5±0.6 d	6.5±0.2 a	18.8±0.6 c	17.9±0.8 b	0.10±0.006 a	0.43±0.02 c	0.81±0.09 a	5.6±0.2 c	7.1±0.2 d

The average number of partial cell profiles examined was 20.
Different letters indicate significant differences between developmental stages in a column for each species separately, at $P \leq 0.05$.
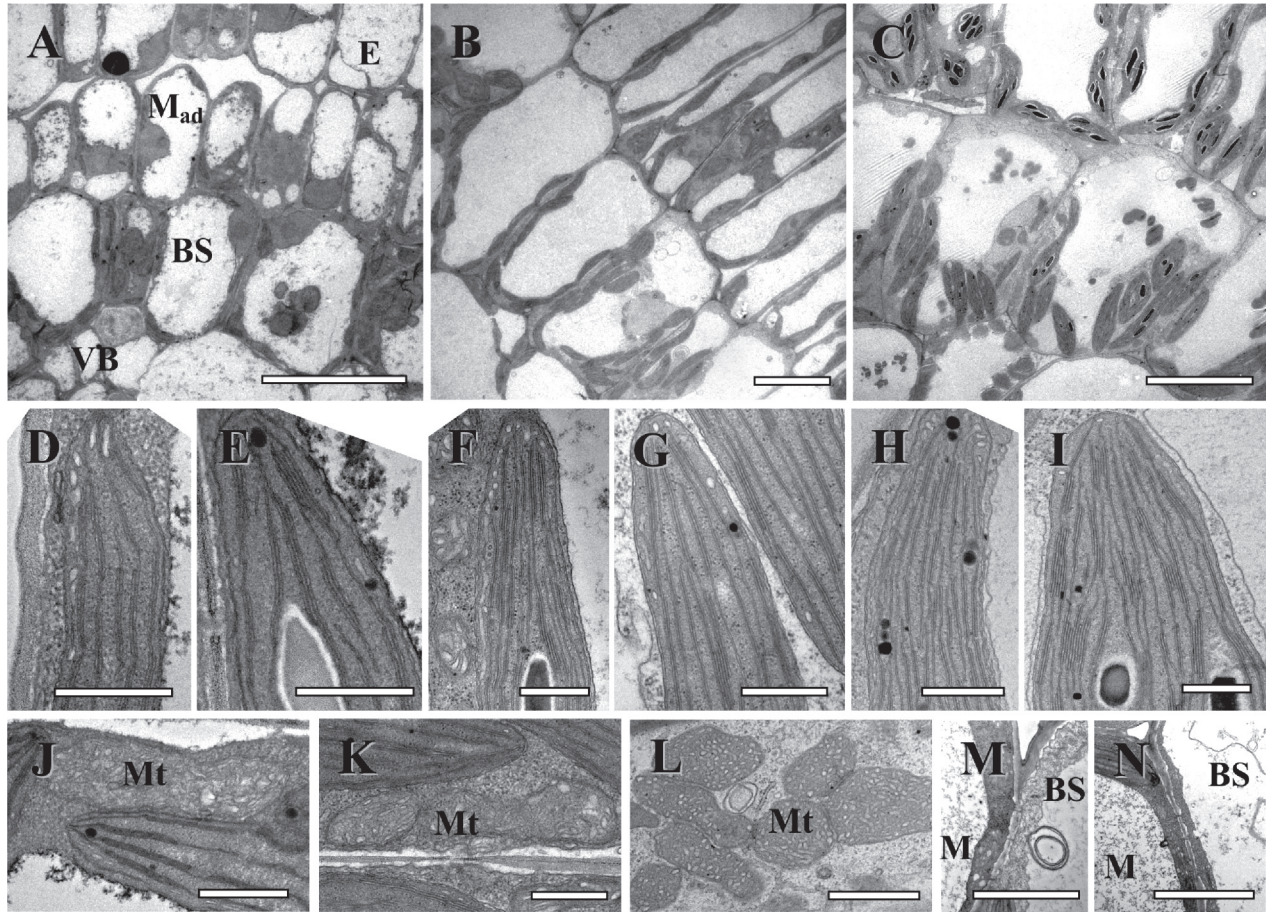
Fig. 2. Electron microscopy of *Cleome angustifolia* longitudinal sections showing three structural stages along the leaf from the base to the tip with the undifferentiated cells at the base, developmental Stage 2 (A, D, E, J), through Stage 3 (B, F, G, K, M), and nearly mature cell structure at the tip, Stage 4 (C, H, I, L, N). (A–C) Micrographs show the development of leaf structure and organelle distribution in BS and M_{ad} cells. (D, F, G) Thylakoid system in M chloroplasts. (E, G, I) Thylakoid system in BS chloroplasts. (J–L) Progression in BS mitochondria ultrastructure specialization and size increase. Note the specific cristae in mitochondria in mature BS cells. (M, N) Plasmodesmata between M and BS cells and BS cell wall thickening. E, epidermis; BS, bundle sheath; M, mesophyll; M_{ad}, adaxial mesophyll; Mt, mitochondria; VB, vascular bundle; WS, water storage tissue. Scale bars=10 μm for A–C; 0.5 μm for D–K; 1 μm for L; 2 μm for M, N.

In Stage 4, observed in the leaf tip (~5.5–6 mm from the base), differentiation of chloroplasts and mitochondria is completed and there is full formation of Glossocardioid-type Kranz anatomy. Chloroplasts of BS cells have numerous grana with 5–15 thylakoids in stacks, while M chloroplasts have poorly developed grana usually with 2–3 thylakoids in stacks (Fig. 2H, I). BS mitochondria are larger and more numerous compared with Stage 3, with cristae showing a distinct tubular structure (Fig. 2L). BS organelles maintain their characteristic positioning in the cell. Also, multiple plasmodesmata connect BS cells with M, as was noted in Stage 3 (Fig. 2N; Table 1). Between Stages 2 and 4, there is not a significant difference in the thickness of the BS cell wall towards the IAS; however, the BS cell walls are about twice as thick as those in M cells (Table 1).

Stages of chlorenchyma development in C. gynandra
Compared with *C. angustifolia*, in *C. gynandra* the basal meristematic zone is extended, with delimitation of BS cells occurring after 1 mm. Development of Kranz anatomy was followed in cross-sections of veins of the highest orders (4 and 5, minor veins) along the longitudinal section from the

base, where cell proliferation occurs, to the tip where BS and M cells are differentiated. While in general the veins differentiate basipetally, the differentiation of neighbouring veins alternates according to their order and timing of initiation, with corresponding changes in development of BS cells. On the other hand, M cells have a clear longitudinal developmental gradient from the base to the tip of the leaf, which is independent of the level of vein and BS differentiation.

At the earliest stages near the base of the leaf, the BS cells are identified by their position adjacent to developing vein tissues, and subsequently by their size and roundish shape (Fig. 1K–N). In Stage 1 (~1–3 mm from the base), anticlinal and radial cell divisions occur in M and BS cells; the two types of cells have nearly the same appearance, with the BS cells being a little wider (Fig. 1L; Table 1). Vascular bundles are not differentiated and they appear as multiplying procambium cells (Fig. 1L).

Recognition of Stage 2 in *C. gynandra* is associated structurally with transition of M cells from division to expansion (~4–5.5 mm from the base). BS cells of the highest order veins are characterized by the vacuoles which are asymmetrically

forming at the centrifugal pole (Figs 1M, 3A) which ulti- mately results in the shift of organelles to the centripetal position in Stage 3. As in *C. angustifolia*, at this stage of development BS and M chloroplasts are enlarged compared with Stage 1 (Table 1) and they have a similar thylakoid sys- tem with numerous small grana (Fig. 3D, E). The mitochon- dria are small with crescent-like cristae (Fig. 3J for BS cell). Most leaf tissues are tightly packed. The BS cell wall is about twice as thick as the M cell wall, and there are multiple plas- modesmata connecting BS and M cells (Table 1). In veins, there is the beginning of differentiation of xylem and phloem elements.

At Stage 3 of development (~5.5–6.5 mm from the base), M and BS cell structural specialization becomes clearer, with well-developed central vacuoles in the M cells and distinc- tive centripetal organelle positioning in BS cells (Figs 1N, 3B). Chloroplasts of both cell types have increased in size (Table 1) and they have a similar level of grana development (Fig. 3F, G). Bundle sheath mitochondria have increased in number and are localized towards the inner cell wall (Fig. 3L). At this stage, the BS cell walls have continued to thicken and there is no change in plasmodesmata number per unit of cell wall length between the M and BS (Fig. 3M;

Table 1). Also, differentiation of 2–3 xylem tracheary ele- ments and first phloem sieve elements has occurred at this stage of development.

In Stage 4, at the leaf tip (~6.5–7 mm from the base), the Atriplicoid type of Kranz anatomy is fully developed. The size of M and BS cells and chloroplasts increased (Table 1). The ultrastructural dimorphism of the chloroplast and mitochon- dria has formed. Chloroplasts of M cells usually have 2–3 thy- lakoids in grana stacks, while BS chloroplasts have numerous grana with 4–10 thylakoids in stacks (Fig. 2H, I). BS cells have abundant, large mitochondria with distinct tubular cristae (Fig. 3N). The BS cell wall facing the IAS is four times thicker than in M; the numbers of plasmodesmata between the M and BS are similar to those in Stage 3 (Fig. 3O; Table 1).

Stomatal initiation from epidermal cells occurred along the longitudinal leaf gradient, with a clear progression in the portion of fully differentiated stomata from the base to mid- region to the tip which was similar for the two species (8, 26, and 72%, respectively, in *C. angustifolia* and 5, 33, and 69%, respectively in *C. gynandra*) (Supplementary Fig. S1 avail- able at *JXB* online). Supplementary Fig. S1 shows images of the abaxial surface of the leaves (results were similar for the adaxial surface, not shown).
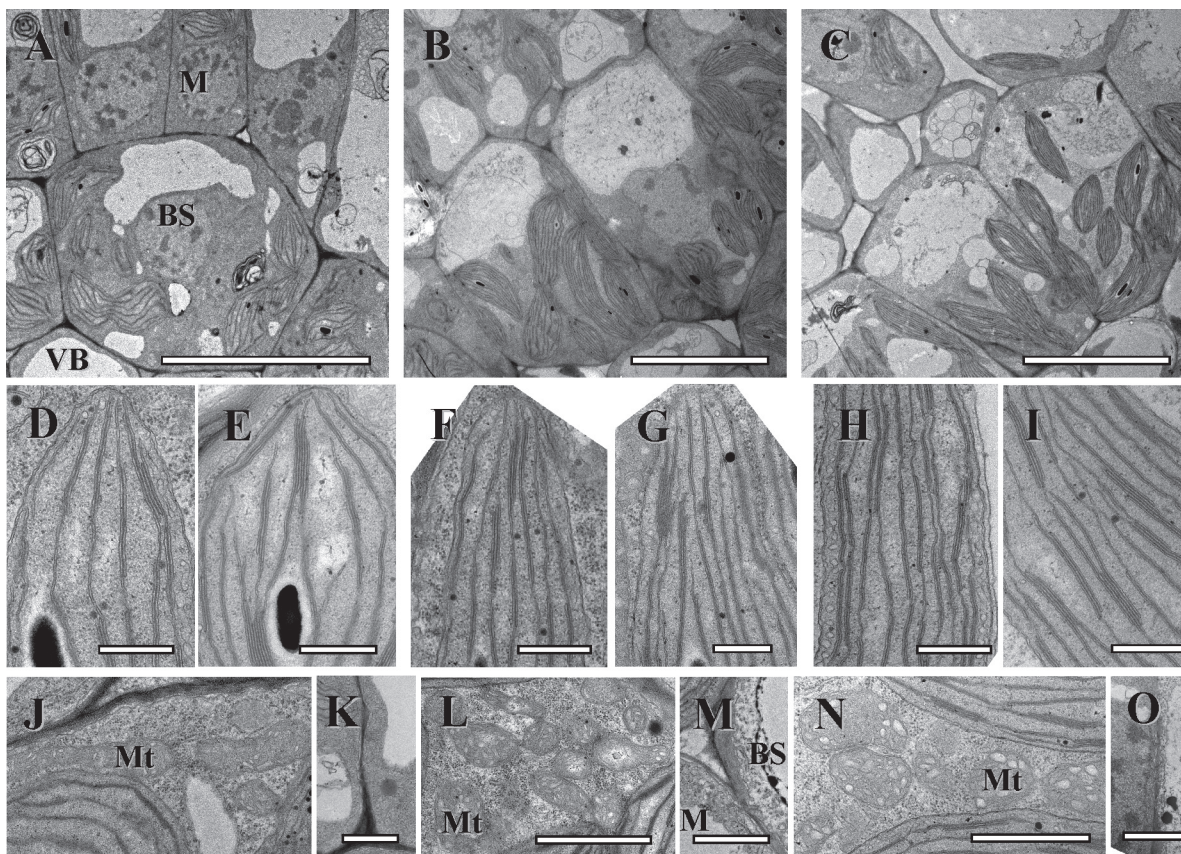

Fig. 3. Electron microscopy of *Cleome gynandra* longitudinal sections showing three structural stages along the leaf from the base to the tip, with the undifferentiated cells at the base, Stage 2 (A, D, E, J, K), through Stage 3 (B, F, G, L, M), and nearly mature cell structure at the tip, Stage 4 (C, H, I, N, O). (A–C) Micrographs show the development of leaf structure and organelle distribution in BS cells. (D, F, H) Thylakoid system in M chloroplasts. (E, G, I) Thylakoid system in BS chloroplasts. (J, L, N) Progression in BS mitochondria ultrastructure specialization and size increase. Note the specific cristae in mitochondria in mature BS cells. (K, M, O) Plasmodesmata between M and BS cells and BS cell wall thickening. BS, bundle sheath; M$_{ad}$, adaxial mesophyll; Mt, mitochondria; VB, vascular bundle. Scale bars=10 μm for A–C; 0.5 μm for D–I; 1 μm for J–O.

Immunolabelling along the developmental gradient

The pattern of PEPC, Rubisco LSU, and GDC expression was studied on longitudinal sections of intermediate size leaves (~6–7 mm) using the reflected/scanning mode of confocal microscopy. The more precise immunogold technique by TEM was used to analyse the base, mid-region, and tip of the same leaf to evaluate the density of labelling in cellular compartments.

In both *Cleome* species, Rubisco is strongly associated with BS chloroplasts from Stage 1 when M and BS cells become distinguishable (Figs 4A, C, 5). Rubisco is suppressed not only in chloroplasts in M cells adjacent to BS (M_{ad} and M_{ab}), but also in the SM cells which are not in contact with the BS cells (Figs 4G, H, 5). Rubisco accumulation per BS chloroplast area reaches a maximum level in Stage 3 (Figs 4B, H, 5), and maintains a high level in Stage 4 at the tip of leaves (Figs 4C, I, 5).

In both species there is selective labelling of GDC in BS mitochondria in Stage 1. In *C. angustifolia* GDC expression increases and reaches a maximum at Stage 2 of development, which is well before BS cell differentiation and mitochondrial structural specialization. In *C. gynandra* a steady increase of GDC was shown in parallel with an increase in BS Rubisco levels (Fig. 5) and cell structural maturation.

PEPC was not detected by immunolocalization in Stage 1 (not shown). In Stage 2, at the confocal microscopy level, there is very low M-specific labelling for PEPC in both *Cleome* species (Fig. 4D, J). The TEM level shows a low and comparable amount of PEPC selectively localized in M_{ad} cells and in both M_{ab} and SM cells (Fig. 5). Both methods show steady accumulation of PEPC preferentially in M cells, with levels reaching a maximum at the tip of the leaf (Stage 4) with little or no difference in particle density between M_{ab} cells adjacent to BS and the SM layers (Figs 4E, F, K, L, 5). Compared with the M_{ad} cells, the expression of PEPC begins earlier in the M_{ab} and SM cells, and usually the density of labelling is higher in these cells at all stages of leaf development (Fig. 5). For *C. gynandra*, comparative counting of the number of particles in the M cells located around the neighbouring veins of different order (with a different level of BS differentiation) shows no difference (not shown).

Western blot analysis

Western blots were performed on extractions of total soluble proteins from individual leaves (young leaves of different lengths, 1–3, 3–6, 6–10, and 10–15 mm, and mature leaves, 30–35 mm) (Fig. 6). Proteins for the C_3 pathway (Rubisco), C_4 cycle (PEPC, PPDK, and NAD-ME), and photorespiratory pathway (GDC) were analysed and represented quantitatively (on a soluble protein basis). The youngest leaves (1–3 mm) of both *Cleome* species contain 22–26% of Rubisco (LSU) compared with the mature stage, with a slow increase in leaves up to 6–10 mm long and a large increase thereafter. The youngest leaves (1–3 mm) of *C. gynandra* contain a low amount of C_4 enzymes; only 12% of PEPC, 6% of PPDK, and 8% of NAD-ME compared

with mature leaves on a soluble protein basis; there was a slow rise in levels in leaves up to 10 mm long, and a large increase thereafter. In contrast, the youngest leaves of *C. angustifolia* have a high amount of C_4 enzymes which on average is 40% of that in the mature stage, with increasing levels as leaf age progressed. The level of GDC shows a steady increase from the youngest up to mature leaves, with higher expression in *C. gynandra* than in *C. angustifolia* (Fig. 6).

CO_2 compensation point, dark respiration, and carbon isotope composition in C. gynandra

Γ and R_d were measured at 10, 20, and 40% O_2 in young (~7 mm) and mature leaves of *C. gynandra* (Fig. 7). Γ was insensitive to increases in O_2 in both; however, the mean value of Γ across all O_2 levels was higher in the young (13.7 ± 1.7 µbar) than in mature leaves (2.6 ± 0.8 µbar). Rates of R_d were higher in young than in mature leaves, with mean values across O_2 levels of 2.91 ± 0.33 in young versus 0.91 ± 0.08 µmol m^{-2} s^{-1} in mature leaves. Excised leaves of *C. angustifolia* were unstable in the leaf chamber, so it was not possible to obtain steady-state readings with the mass spectrometer. Values of carbon isotope composition ($\delta^{13}C$) measured from leaf sections of *C. gynandra* at the base, tip, and middle of young leaves were –14.1 (±0.03), –14.1 (±0.02), and –14.7 (±0.08), respectively, compared with –14.6 (±0.12) in mature leaves.

Discussion

Origin of M and BS cells in C_4 Cleome

Cleome angustifolia and *C. gynandra* have compound leaves with a similar pattern of initiation, but with distinct differences in the patterns of minor veins and Kranz anatomy spatial development. In *C. angustifolia*, which has a form of Kranz (called Glossocardioid) that consists of a single complex unit, M and BS cells originate from subepidermal layers of ground meristem during leaflet initiation. The pattern of origins of M and BS cells is very close to that in *S. taxifolia* which has Schoberioid-type anatomy with a similar positioning of two chlorenchyma layers at the leaf periphery (Koteyeva *et al.*, 2011a). In *C. gynandra*, which has Atriplicoid-type anatomy with Kranz units around individual veins, the BS cells towards the adaxial side are sister to procambium cells arising from the adaxial derivative of the first periclinal division of the ground meristem cell (the abaxial derivative gives rise to the procambium initial). The rest of the BS cells ontogenetically originate from the ground meristem cells of the second, third, and fourth layers adjacent to the vein. M cells are also derived from the ground meristem having different ontogeny, namely subepidermal and central cells, which is similar to that of *A. rosea* with Atriplicoid-type anatomy (Liu and Dengler, 1994). In both *C. angustifolia* and *C. gynandra* it is difficult to reveal the progenitor cells of the shoot apical meristem due to initiation of leaflets from the primary primordium which is the future petiole. As shown
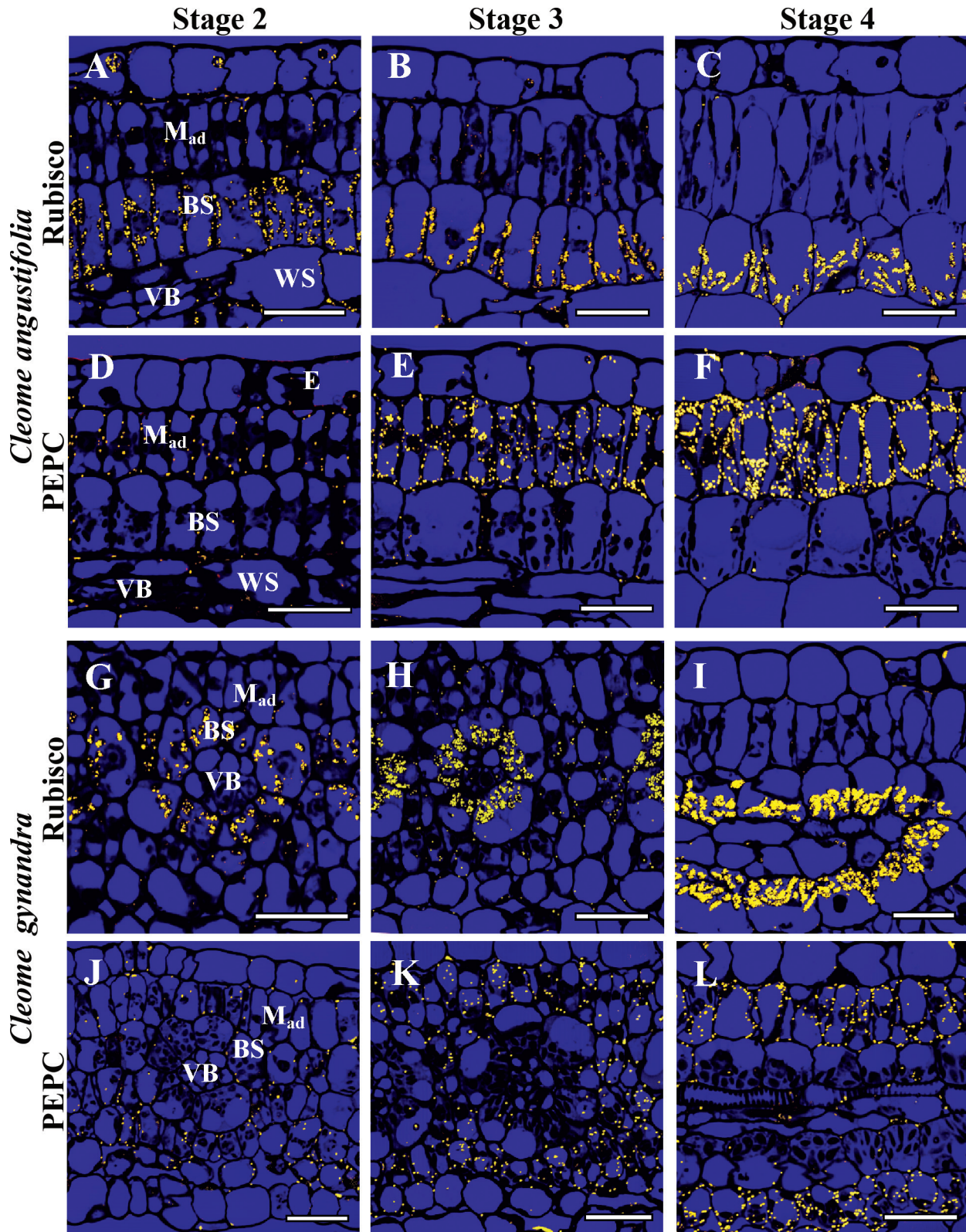
Fig. 4. *In situ* immunolocalization of Rubisco LSU (A–C, G–I) and PEPC (D–F, J–L) in leaves of *Cleome angustifolia* (A–F) and *C. gynandra* (G–L) at three developmental stages. Reflected/transmitted confocal imaging of longitudinal leaf sections shows Rubisco LSU selectively localized to BS cells beginning from developmental Stage 2 (A, G); note labelling in the few chloroplasts in the epidermis and water storage cells (A). The weak labelling for PEPC is M specific from the earliest stages (D, J), with increased labelling beginning from Stage 3 (E, K). At Stage 4, high labelling for Rubisco and PEPC is partitioned to BS and M, respectively. BS, bundle sheath; E, epidermis; M_{ad}, adaxial mesophyll; VB, vascular bundle, WS, water storage. Scale bars=20 μm for A–L.
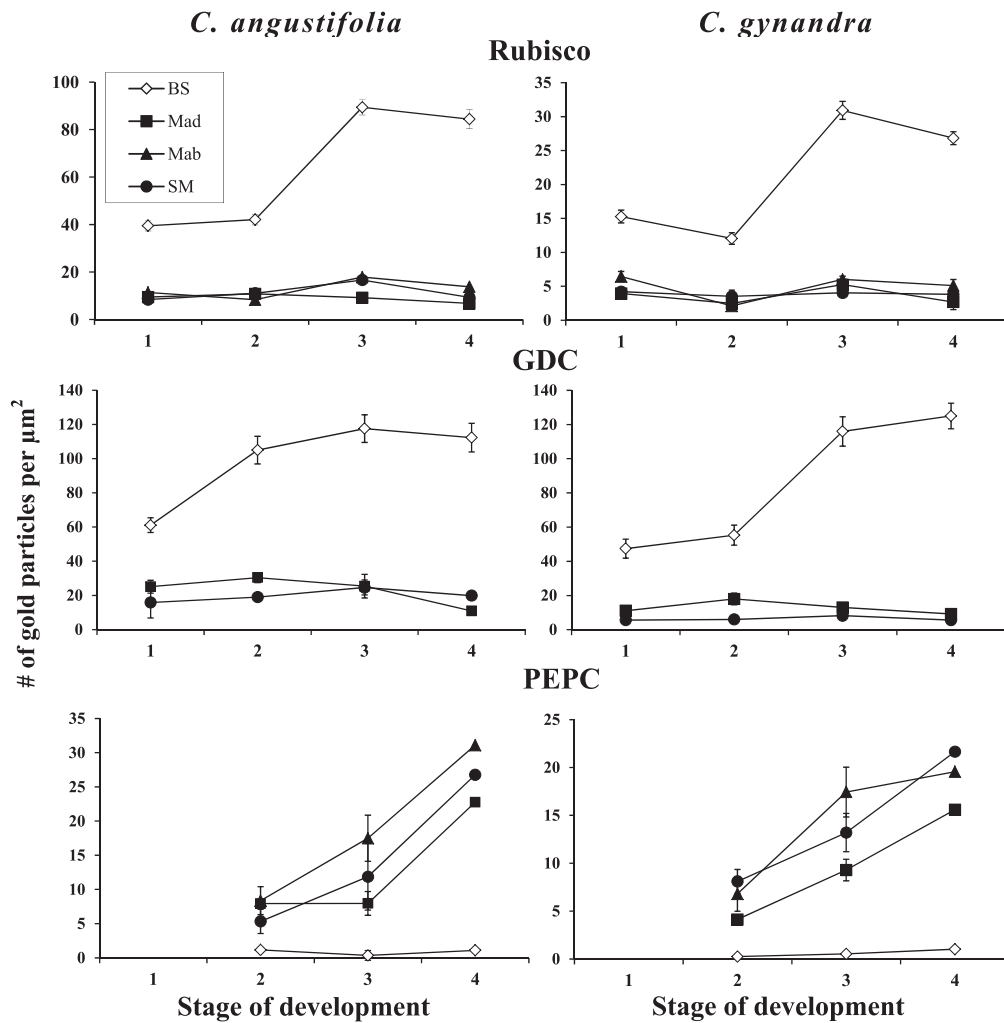
Fig. 5. Graphical representation showing the density of immunolabelling for Rubisco LSU (top panels) in BS versus M chloroplasts, GDC (middle panels) in BS versus M mitochondria, and PEPC (bottom panel) in BS versus M cytosol at four stages of leaf development for *Cleome angustifolia* and *C. gynandra*. Also, the comparison was made between three types of M cells: M_{ad}, adaxial mesophyll; M_{ab}, abaxial mesophyll cells which are in contact with the BS cells; and SM (spongy mesophyll), an additional M layer on the abaxial side of the leaf which does not have contact with BS. In both graphs, the *y*-axis represents the number of gold particles per μm^2 of chloroplast, mitochondria, or cytosol area, and the *x*-axis represents the developmental stages. For each cell type and stage of development, 10–15 cell areas were used for counting. BS, bundle sheath; M, mesophyll.

in previous studies, the ontogenetic origin of M and BS cells has no effect on the structural, biochemical, and functional peculiarities of C₄ tissues which shows a clear convergent evolution of a highly coordinated functioning of the two-cell system (Dengler *et al.*, 1985, 1986, 1996; Koteyeva *et al.*, 2011a).

Longitudinal patterns of development in C₄ Cleome

The form of Kranz in leaves of *C. angustifolia* allows all stages of the developmental progression to be studied along one file of chlorenchyma cells from the base to the tip of an intermediate size leaf. A similar basipetal pattern of development along a single lineage of cells has also been observed in two other forms having a single compound Kranz unit (Schoberioid and Salsinoid type in family Chenopodiaceae, Koteyeva *et al.*, 2011a), and in several C₄ monocots with parallel venation (Langdale *et al.*, 1988a; Soros and Dengler, 2001; Wakayama *et al.*, 2003; Li *et al.*, 2010; Majeran *et al.*, 2010; Nelson, 2011).

In contrast to *C. angustifolia*, development of Kranz anatomy in leaves of *C. gynandra* is closely associated with vein differentiation. Having in general a longitudinal basipetal pattern, the initiation of minor veins is sequential in time. Veins at different stages of differentiation in *C. gynandra*, which are alternate in the longitudinal section, can be easily recognized by size, anatomy, chloroplast ultrastructure, and accumulation of Rubisco in the BS cells. The pattern of vascular development in *C. gynandra*, and associated progression in specialization of BS cells, resembles that described for C₄ *A. rosea* (Dengler *et al.*, 1995), C₄ *A. hypochondriacus* (Wang *et al.*, 1993), and C₄ *Flaveria trinervia* (McKown and Dengler, 2009).

Stages of C₄ development along the leaf

Irrespective of having vastly different Kranz anatomical types, *C. angustifolia* and *C. gynandra* have a similar
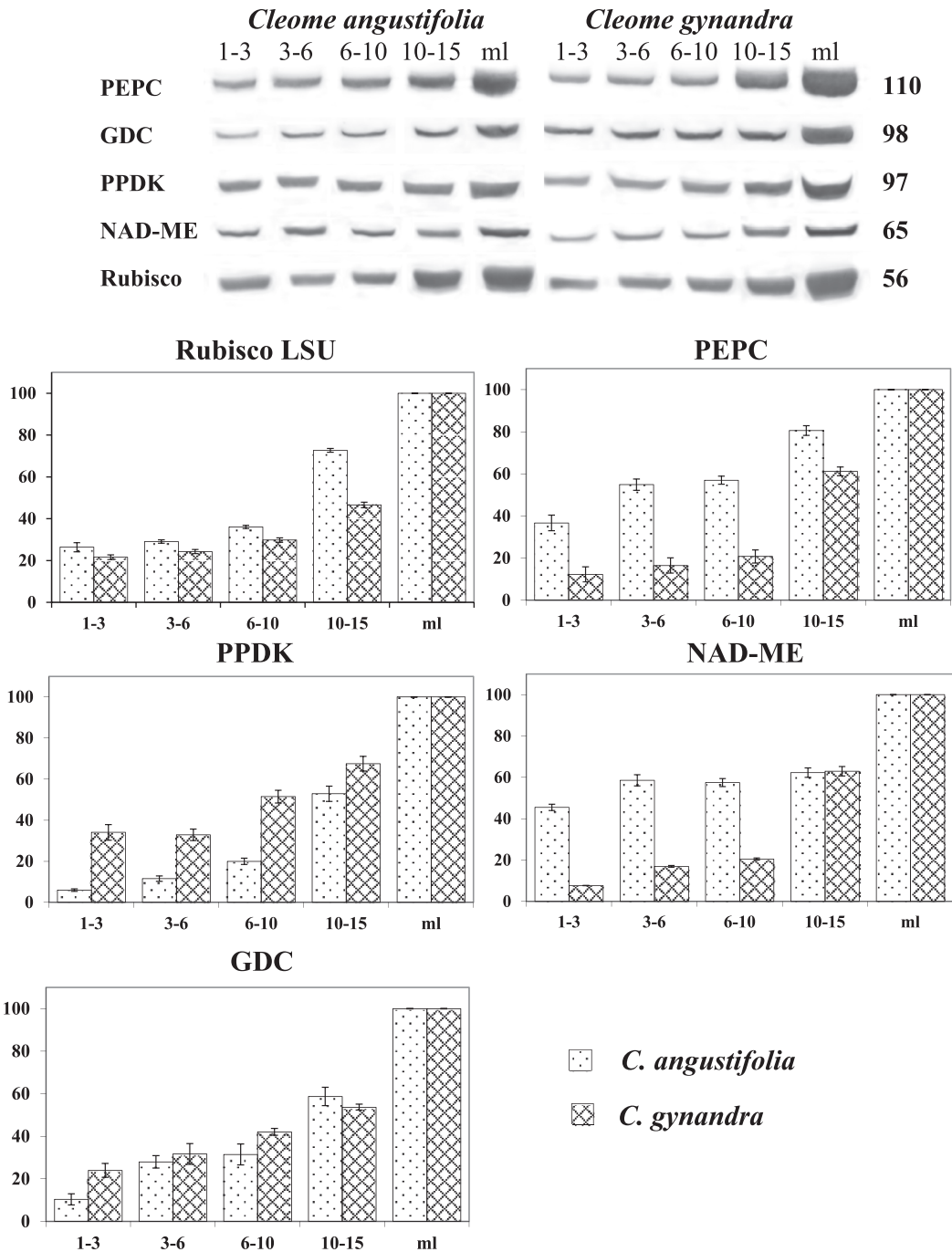
Fig. 6. Western blot analysis showing accumulation of C$_4$ enzymes, GDC, and Rubisco LSU during leaf development in two *Cleome* species. Total soluble proteins were extracted from individual leaves of different lengths of *C. angustifolia* and *C. gynandra*. Blots were probed with antibodies raised against PEPC, GDC, PPDK, NAD-ME, and Rubisco LSU. Top: representative western blots showing detection of each protein. Numbers on the right indicate molecular mass in kilodaltons. Bottom: quantitative representation of western blot data. 100% on the *y*-axis refers to the level achieved in mature leaves. The *x*-axis represents the length of the leaves.

sequence of events during C$_4$ leaf development. However, the lengths of the zones along the leaves where transitions occur are different between the two species, which may be related to differences in anatomy or growth rates. Four notable stages in C$_4$ development were recognized from base to tip of young leaves of both species based on anatomical and ultrastructural features (illustrated in Fig. 8).

Structural development

Stage 1, the beginning of Kranz, is distinguished by M and BS cells which are positionally delimited from meristem precursors, performing anticlinal/radial divisions and having similar shape and structure with ultrastructurally uniform organelles. In Stage 2 there is expansion of M and BS cells, vacuoles are developing, and chloroplasts and mitochondria are replicating and enlarging. The plasmodesmata frequency
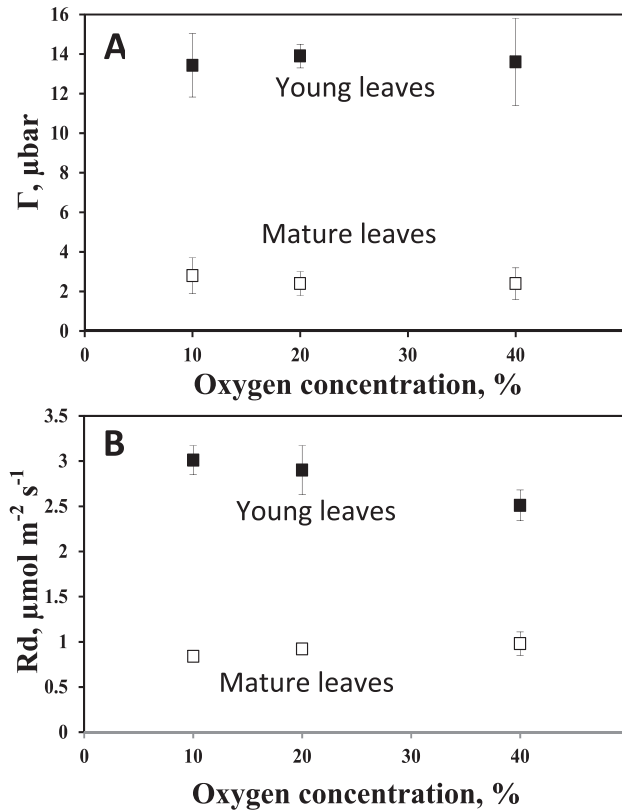
Fig. 7. The effect of oxygen on the CO$_2$ compensation point (Γ; A) and dark respiration (R_d; B) in young and mature leaves of *Cleome gynandra*. Number of replications n=5–8 for young leaves and n=3–6 for mature leaves. One-way analysis of variance shows that varying O$_2$ had no significant effect on Γ or R_d in young or mature leaves.

between M and BS cells is also high at this time. In Stage 3, structural specialization of M and BS begins. The M cells develop a palisade-like shape with a large central vacuole and organelles around the cell periphery. Organelles in BS cells become localized in a centripetal position towards the inner cell wall characteristic of mature Kranz anatomy in C$_4$ *Cleome* species. The chloroplasts, and the mitochondria, between M and BS cells are structurally similar, indicating an immature stage of development. In Stage 4, full Kranz anatomy has developed, with structurally specialized dimorphic chloroplasts and mitochondria in M and BS cells.

There were some structural parameters which show a continuous change along the leaf gradient. In both species there was an increase in the sizes of M and BS cells, chloroplasts, and mitochondria, and in stomatal development and density (illustrated on the left side of Fig. 8). There was an increase in the length of the M cells with no change in width, while there was an ~2-fold increase in both the length and width of the BS cells. During development there is continual enlargement of M and BS chloroplasts, with an increase in length by ~3-fold in both species. The density of plasmodesmata at the interphase between M and BS cells increases or remains constant (see Table 1) despite the increase in size of M and BS cells (and contact between the two) due to the formation of secondary plasmodesmata during development. This indicates establishment of symplastic connections between M and BS from the earliest stages of development which enables intercellular movement of metabolites for C$_4$ photosynthesis. In both species, BS cell wall thickening, which starts soon after the BS cell become positionally delimited, is considered
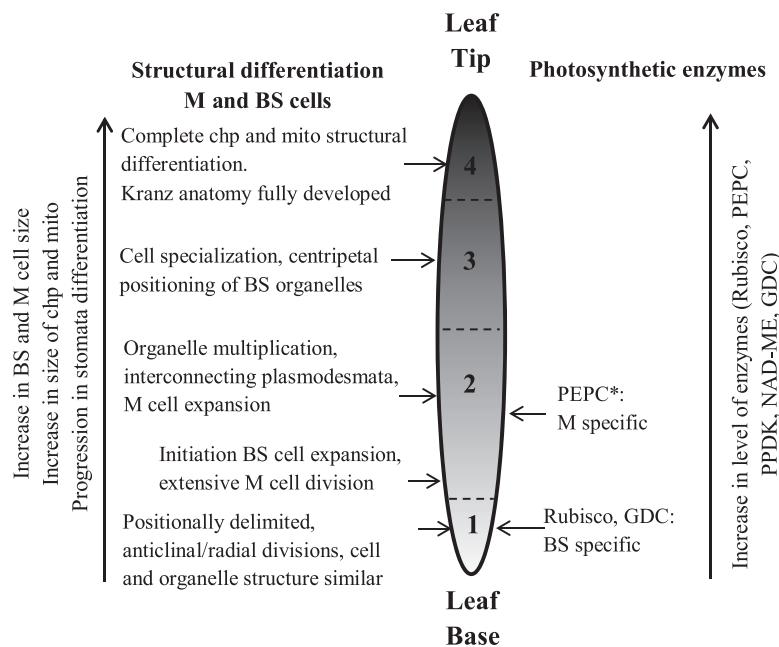

Fig. 8. Illustration of major changes during development of C$_4$ photosynthesis in *Cleome angustifolia* and *C. gynandra* from the basal region to the tip of young leaves. The numbers refer to four stages of chlorenchyma development; see text for the corresponding length of the zones for each species. The horizontal arrows point to specific changes occurring in each of the four stages. The vertical arrows indicate continual changes which occur along the longitudinal gradient. BS, bundle sheath, chp, chloroplasts; GDC, glycine decarboxylase; M, mesophyll; mito, mitochondria. *PEPC was selectively localized to M cells in stage 2 (there was insufficient labelling to determine its localization by immunolocalization in stage 1).

to contribute to diffusive resistance and limit CO_2 leakage from the BS during C_4 photosynthesis (von Caemmerer and Furbank, 2003).

Biochemical development

In both species there is a very early cell-specific C_4-like pattern of enzyme accumulation. BS cells complete divisions, and initiate cell expansion with multiplication of chloroplasts and mitochondria earlier than M cells which continue to have active anticlinal divisions up to Stage 2. However, biochemical specialization in M and BS begins simultaneously from the meristematic zone in Stage 1. Rubisco and GDC are selectively expressed in chloroplasts and mitochondria, respectively, in BS cells, and at the same time they are suppressed in chloroplasts and mitochondria of the M cells, characteristic of the C_4 system. So, while organelles, chloroplasts and mitochondria, do not become ultrastructurally differentiated in BS and M until full maturation of Kranz, biochemical specialization of organelles in the two chlorenchyma cells is occurring already in the meristematic stages right after the layers become positionally delimited. This shows that Rubisco and GDC expression in these two *Cleome* species is not directly associated with structural differentiation of M and BS cells.

Early cell-specific Rubisco expression during leaf development has also been observed in several other C_4 species, including *Arundinella hirta* (Wakayama *et al.*, 2003), *A. rosea* (Dengler *et al.*, 1995), *S. eltonica*, and *S. taxifolia* (Koteyeva *et al.*, 2011a). In contrast, a C_3 default state with Rubisco appearing initially in both M and BS chloroplasts has been observed in other C_4 species, with selective expression of Rubisco in BS depending on light or developmental cues in maize (Sheen and Bogorad, 1985; Langdale *et al.*, 1988b; Sheen, 1999), in *A. hypochondriacus* (Patel and Berry, 2008), in three structural forms of C_4 in family Cyperaceae (Soros and Dengler, 2001), and in *Salsola richteri* (Voznesenskaya *et al.*, 2003b). Clearly these differences in transitions to C_4 suggest evolution of alternative cues for initiation of C_4 development; although there may be convergence in factors (transcriptional or transacting) controlling synthesis of components of the C_4 system.

PEPC levels were too low to detect in Stage 1. From its earliest detection in Stage 2, it was M specific and the level increased in parallel with M differentiation. In a number of other developmental studies, PEPC gene expression also appears to be initially M specific and increased depending on M differentiation (Langdale *et al.*, 1988a; Dengler *et al.*, 1995; Stockhaus *et al.*, 1997; Soros and Dengler, 2001; Wakayama *et al.*, 2003; Koteyeva *et al.*, 2011a).

The results in both C_4 *Cleome* species indicate that intercellular compartmentation for C_4 photosynthesis is established early without a C_3 default state, that enzyme levels to support the C_4 system continue to rise during the four stages of leaf development, and that structural positioning of organelles and differentiation of chloroplasts and mitochondria occur later (Fig. 8). This suggests that development of C_4 biochemistry may be a driver for organelle differentiation, namely for M and BS chloroplasts to provide the balance in ATP and NADPH from photochemistry to support the NAD-ME-type C_4 cycle (see Edwards and Voznesenskaya, 2011), and

for mitochondria to provide the capacity for transport and metabolism to support decarboxylation via NAD-ME. The same pattern of development in these two C_4 *Cleome* species which have very different types of Kranz anatomy and independent evolutionary lineages is consistent with the concept that genes to support the C_4 cycle were already primed for recruitment and selective expression in M and BS cells (Brown *et al.*, 2011; Kajala *et al.*, 2012).

A functional analysis of young versus mature leaves of *C. gynandra* was made by analysing the effect of O_2 on Γ to determine if the response is indicative of C_4, intermediate, or C_3 photosynthesis. C_4 plants have very low Γ (1–5 µbar) while C_3 plants have high values of Γ (~40–50 µbar at 25 °C and 20% O_2). Additionally, Γ in C_4 plants has little or no sensitivity to O_2, while values in C_3 plants approximately double with a 2-fold increases in O_2. C_3–C_4 species have intermediate Γ values, which increase with the level of O_2 (Krenzer *et al.*, 1975; Brooks and Farquhar, 1985; von Caemmerer, 1989, 2000; Ku *et al.*, 1991; Vogan *et al.*, 2007; Voznesenskaya *et al.*, 2007). Mature leaves of *C. gynandra* show a clear C_4-type response, with values of Γ of ~2.5 µbar with insensitivity to O_2. In young leaves, the lack of sensitivity of Γ to O_2, between 10% and 40%, is characteristic of C_4 plants. The higher Γ values in young leaves (~14 µbar) are probably due to the higher R_d and lower V_{cmax} for Rubisco (see western blots), due to the dependence of Γ on the R_d/V_{cmax} ratio (von Caemmerer, 2000), in addition to its dependence on Rubisco kinetic properties and the level of photorespiration. In plant leaves, R_d saturates at relatively low levels of O_2 (~2–3% O_2), whereas the reaction of O_2 with RuBP oxygenase, in competition with CO_2, results in an increase in Γ in response to higher levels of O_2. Thus, in the absence of R_d, extrapolated plots of Γ versus O_2 would intercept at zero, whereas contribution from R_d results in the intercept on the *y*-axis (Brooks and Farquhar, 1985). Thus, the results suggest that young leaves of *C. gynandra* are functionally C_4. A factor which may minimize the occurrence of photorespiration and maintain a lower Γ in young leaves is the selective localization of photosynthetic enzymes to M and BS cells for function of C_4 early in development. Also, the selective localization of GDC to the BS indicates the presence of conditions favourable for refixation of photorespired CO_2 around Rubisco from the very early stages of development. As leaves develop, there is an increase in the level of GDC in the two *Cleome* species; this may be associated with multiplication and increase in size of BS mitochondria (where GDC is localized), which was observed during development along a longitudinal gradient in young leaves (Stage 3). There is the possibility that sensitivity of photosynthesis to O_2 occurs at the base of young leaves, but its contribution to carbon assimilation is expected to be very low (due to low Rubisco, and undeveloped stomata).

Expression of C_4 enzymes in M cells which do not have contact with the BS

Both *Cleome* species have an additional layer of chlorenchyma cells on the abaxial side of leaves (SM) which is ontogenetically related to the abaxial M layer which is adjacent to the

BS. They are not associated with BS, and structurally resemble M cells with well-developed chloroplasts. It was shown by confocal immunohistochemistry and TEM immunogold labelling that their cytosol contains PEPC at a similar level to that of adaxial and abaxial M cells which are in contact with BS. The expression of Rubisco and GDC in these distal M cells is suppressed, and structural and biochemical differentiation of these cells occurs in parallel with the M cells in contact with BS.

There are not many cases where C$_4$ plants have more than two M cells between neighbouring BS cells; analysis of 119 C$_4$ grasses (Hattersley and Watson, 1975) showed that no M cell is separated from the nearest BS cell by more than one other M cell (the maximum cell distant count). Based on studies with maize, it has long been considered that M cells differentiate to form a C$_4$-type cell only when they are in contact with BS; and that M cells distant from BS are deprived of PEPC expression and contain Rubisco in chloroplasts (Langdale *et al.*, 1988b). In maize husk having >20 additional cells between BS cells, the structural and biochemical specialization for C$_4$ was shown only in M cells which are in contact with BS cells, which supports this hypothesis (Langdale *et al.*, 1988b; Pengelly *et al.*, 2011). Also, in *A. rosea* there is an extra layer of abaxial and adaxial cells which are not in contact with the BS cells; Dengler *et al.* (1995) found that PEPC expression was restricted to the M cells adjacent to BS cells along the whole maturation gradient. However, the authors noted that those cells contain few organelles and are non-photosynthetic (hypodermal cells, probably functioning in water storage). Thus, the results with the two C$_4$ *Cleome* species, which clearly shows formation of C$_4$-type M cells which are not adjacent to the BS, is an interesting variation on regulation of C$_4$ development.

Signalling for tissue-specific development of BS and M cells

Veins in C$_4$ plants have been considered to play an organizing role in the differentiation of Kranz anatomy as a source of the positional signal which controls the coordinated development of at least two cells in a radius around individual veins, as in *C. gynandra*, generating the pattern of Vein–BS–M–M–BS–Vein units (Langdale *et al.*, 1988*a*, *b*; Nelson and Langdale, 1992; Langdale, 2012) and candidate genes which may be associated with differentiation of Kranz anatomy have been proposed (Wang *et al.*, 2013). This is a logical hypothesis for the leaf structures where the anatomy consists of multiple simple Kranz units around individual veins which occur in many C$_4$ lineages coupled with increased leaf venation during evolution from C$_3$ to C$_4$ species (McKown and Dengler, 2007; Griffiths *et al.*, 2013). However, the pattern of development of Kranz anatomy in the *Cleome* species in the current study is not compatible with this hypothesis. In *C. gynandra*, which has Atriplicoid-type anatomy, the structural development of M specialization is not correlated with BS cell development. Rather BS cell development is correlated with stages of differentiation of alternate veins, but not the M cells which have only a basipetal gradient of maturation. Also, the hypothesis

of signalling from vascular tissue to control differentiation of the M cells adjacent to BS cells is not consistent with the same expression pattern of C$_4$ in the cells of the abaxial SM layer not adjacent to BS. These two abaxial M layers represent sister cells which originated from the division of the abaxial subepidermal ground meristem; but, their segregation occurs before, or simultaneously with, the start of procambial strand initiation. One could imagine that the 'M' signal may come to the progenitor cell before its division, which could explain the existence of PEPC in both M layers; but, in this case, the signal cannot come from the undifferentiated vein. Also, the selective expression of PEPC in the M cells occurs later, during Stage 2, while the selective expression of Rubisco and GDC occurs during Stage 1, which suggests temporal differences in signalling.

With respect to *C. angustifolia*, recently it was shown that evolution of C$_4$ species having a single compound Kranz unit in C$_4$ *Salsola* occurs not with increasing vein density, but by increased succulence and development of a layer of BS cells around veins and water storage tissue (Voznesenskaya *et al.*, 2013). For differentiation of tissue for this type of anatomy, veins could not be the centre for a positional signal since they are not evenly distributed relative to the position of Kranz anatomy, and their contact with BS is not essential (Koteyeva *et al.*, 2011*a*). The spatial positioning of M and BS cells relative to each other, unlike the positioning of Kranz around individual veins, is essential to the mechanism controlling their differentiation.

Concluding remarks

The results indicate that two C$_4$ *Cleome* species, which have different Kranz anatomy and evolved independently in family Cleomaceae, have a similar developmental pathway for C$_4$ during structural and biochemical maturation. The ontogenetic programme for this development involves control of cell-specific patterns of mitosis (rates and plane) and cell expansion, division of chloroplasts and mitochondria, structural differentiation and spatial distribution, cell wall modification, and plasmodesmata formation, with all of these characteristics occurring in close coordination with vascular system differentiation. The early partitioning of Rubisco, GDC, and PEPC expression between M and BS in both species shows that factors controlling their cell specificity must be activated as soon as the tissue become delimited. Further regulation occurs during development, with increased levels of expression of photosynthetic enzymes, and structural differentiation of M and BS cells and organelles. The results provide insight into stages to consider for transcriptome and proteomic studies to search for candidate genes which control structural and biochemical transitions in C$_4$ development.

Supplementary data

Supplementary data are available at *JXB* online.

Figure S1. Scanning electron microscopy of the abaxial surfaces of the young leaves of *Cleome angustifolia* (6 mm)

and *C. gynandra* (7 mm) showing the level of stomata differentiation in the tip, middle, and base.

Acknowledgements

References

Bräutigam A, Kajala K, Wullenweber J, et al. 2011. An mRNA blueprint for C_4 photosynthesis derived from comparative transcriptomics of closely related C_3 and C_4 species. *Plant Physiology* **155,** 142–156.

Brooks A, Farquhar GD. 1985. Effect of temperature on the CO_2/O_2 specificity of ribulose-1,5-bisphosphate carboxylase/oxygenase and the rate of respiration in the light. *Planta* **165,** 397–406.

Brown NJ, Newell CA, Stanley S, Chen JE, Perrin AJ, Kajala K, Hibberd JM. 2011. Independent and parallel recruitment of preexisting mechanisms underlying C_4 photosynthesis. *Science* **331,** 1436–1439.

Brown WV. 1975. Variations in anatomy, associations, and origin of Kranz tissue. *American Journal of Botany* **62,** 395–402.

Covshoff S, Knerova J, Burgess SJ, Kumpers BMC. 2013. Getting the most out of natural variation in C_4 photosynthesis. *Photosynthesis Research* **119,** 157–167.

Dengler NG, Dengler RE, Donnelly PM, Filosa MF. 1995. Expression of the C_4 pattern of photosynthetic enzyme accumulation during leaf development in *Atriplex rosea* (Chenopodiaceae). *American Journal of Botany* **82,** 318–327.

Dengler NG, Dengler RE, Hattersley PW. 1985. Differing ontogenetic origins of PCR (Kranz) sheaths in leaf blades of C_4 grasses (Poaceae). *American Journal of Botany* **72,** 284–302.

Dengler NG, Dengler RE, Hattersley PW. 1986. Comparative bundle sheath and mesophyll differentiation in the leaves of the C_4 grasses *Panicum effusum* and *P. bulbosum*. *American Journal of Botany* **73,** 1431–1442.

Dengler NG, Donnelly PM, Dengler RE. 1996. Differentiation of bundle sheath, mesophyll, and distinctive cells in the C_4 grass *Arundinella hirta* (Poaceae). *American Journal of Botany* **83,** 1391–1405.

Dengler NG, Nelson T. 1999. Leaf structure and development in C_4 plants. In: Sage RF, Monson RK, eds. C_4 *plant biology. Physiological ecology series*. San Diego: Academic Press, 133–172.

Edwards GE, Voznesenskaya EV. 2011. C_4 photosynthesis: Kranz forms and single-cell C_4 in terrestrial plants. In: Raghavendra AS, Sage RF, eds. C_4 *photosynthesis and related CO_2 concentrating mechanisms*. Dordrecht, The Netherlands: Springer, 29–61.

Edwards GE, Walker DA. 1983. C_3, C_4: *mechanisms, and cellular and environmental regulation, of photosynthesis*. Oxford: Blackwell Scientific publications.

Esau K. 1965. *Plant anatomy*. New York: Wiley Interscience.

Feodorova TA, Voznesenskaya EV, Edwards GE, Roalson EH. 2010. Biogeographic patterns of diversification and the origins of C_4 in *Cleome* (Cleomaceae). *Systematic Botany* **35,** 811–826.

Griffiths H, Weller G, Toy LFM, Dennis RJ. 2013. You're so vein: bundle sheath physiology, phylogeny and evolution in C_3 and C_4 plants. *Plant, Cell and Environment* **36,** 249–261.

Hatch MD. 1987. C_4 photosynthesis: a unique blend of modified biochemistry, anatomy and ultrastructure. *Biochimica et Biophysica Acta* **895,** 81–106.

Hattersley PW, Watson L. 1975. Anatomical parameters for predicting photosynthetic pathways of grass leaves: 'the maximum lateral count' and 'the maximum cells distant count'. *Phytomorphology* **25,** 325–333.

Kajala K, Brown NJ, Williams BP, Borrill P, Taylor LE, Hibberd JM. 2012. Multiple *Arabidopsis* genes primed for recruitment into C_4 photosynthesis. *The Plant Journal* **69,** 47–56.

Koteyeva NK, Voznesenskaya EV, Berry JO, Chuong SDX, Franceschi VR, Edwards GE. 2011a. Development of structural and biochemical characteristics of C_4 photosynthesis in two types of Kranz anatomy in genus *Suaeda* (family Chenopodiaceae). *Journal of Experimental Botany* **62,** 3197–3212.

Koteyeva NK, Voznesenskaya EV, Roalson EH, Edwards GE. 2011b. Diversity in forms of C_4 in the genus *Cleome* (Cleomaceae). *Annals of Botany* **107,** 269–283.

Krenzer EG, Moss DN, Crookston RK. 1975. Carbon dioxide compensation points of flowering plants. *Plant Physiology* **56,** 194–206.

Ku MS, Wu J, Dai Z, Scott RA, Chu C, Edwards GE. 1991. Photosynthetic and photorespiratory characteristics of *Flaveria* species. *Plant Physiology* **96,** 518–528.

Langdale JA. 2012. C_4 cycles: past, present, and future research on C_4 photosynthesis. *The Plant Cell* **23,** 3879–3892.

Langdale JA, Rothermel BA, Nelson T. 1988a. Cellular pattern of photosynthetic gene expression in developing maize leaves. *Genes and Development* **2,** 106–115.

Langdale JA, Zelitch I, Miller E, Nelson T. 1988b. Cell position and light influence C_4 versus C_3 patterns of photosynthetic gene expression in maize. *EMBO Journal* **7,** 3643–3651.

Li P, Ponnala L, Gandotra N, et al. 2010. The developmental dynamics of the maize leaf transcriptome. *Nature Genetics* **42,** 1060–1067.

Liu Y, Dengler NG. 1994. Bundle sheath and mesophyll cell differentiation in the C_4 dicotyledon *Atriplex rosea*: quantitative ultrastructure. *Canadian Journal of Botany* **72,** 644–657.

Long JJ, Berry JO. 1996. Tissue-specific and light-mediated expression of the C_4 photosynthetic NAD-dependent malic enzyme of amaranth mitochondria. *Plant Physiology* **112,** 473–482.

Majeran W, Friso G, Ponnala L, et al. 2010. Structural and metabolic transitions of C_4 leaf development and differentiation defined by microscopy and quantitative proteomics. *The Plant Cell* **22,** 3509–3542.

Marshall DM, Muhaidat R, Brown NJ, Liu Z, Stanley S, Griffiths H, Sage RF, Hibberd JM. 2007. *Cleome*, a genus closely related to *Arabidopsis*, contains species spanning a developmental progression from C_3 to C_4 photosynthesis. *The Plant Journal* **51,** 886–896.

Maxwell K, Badger MR, Osmond CB. 1998. A comparison of CO_2 and O_2 exchange patterns and the relationship with chlorophyll fluorescence during photosynthesis in C_3 and CAM plants. *Functional Plant Biology* **25,** 45–52.

McKown AD, Dengler NG. 2007. Key innovations in the evolution of Kranz anatomy and C_4 vein pattern in *Flaveria* (Asteraceae). *American Journal of Botany* **94,** 382–399.

McKown AD, Dengler NG. 2009. Shifts in leaf vein density through accelerated vein formation in C_4 *Flaveria* (Asteraceae). *Annals of Botany* **104,** 1085–1098.

Muhaidat R, Sage RF, Dengler NG. 2007. Diversity of Kranz anatomy and biochemistry in C_4 eudicots. *American Journal of Botany* **94,** 362–381.

Nelson T. 2011. The grass leaf developmental gradient as a platform for a systems understanding of the anatomical specialization of C_4 leaves. *Journal of Experimental Botany* **62,** 3039–3048.

Nelson T, Langdale JA. 1992. Developmental genetics of C_4 photosynthesis. *Annual Review of Plant Physiology and Plant Molecular Biology* **43,** 25–47.

Newell CA, Brown NJ, Liu Z, Pflug A, Gowik U, Westhoff P, Hibberd JM. 2010. *Agrobacterium tumefaciens*-mediated transformation of *Cleome gynandra* L., a C_4 dicotyledon that is closely related to *Arabidopsis thaliana*. *Journal of Experimental Botany* **61,** 1311–1319.

Patel M, Berry JO. 2008. Rubisco gene expression in C_4 plants. *Journal of Experimental Botany* **59,** 1625–1634.

Pengelly JJL, Kwasny S, Bala S, Evans JR, Voznesenskaya EV, Koteyeva NK, Edwards GE, Furbank RT, von Caemmerer S. 2011. Functional analysis of corn husk photosynthesis. *Plant Physiology* **156,** 503–513.

Peter G, Katinas L. 2003. A new type of Kranz anatomy in Asteraceae. *Australian Journal of Botany* **51,** 217–226.

Ramsperger VC, Summers RG, Berry JO. 1996. Photosynthetic gene expression in meristems and during initial leaf development in a C$_4$ dicotyledonous plant. *Plant Physiology* **111,** 999–1010.

Ruuska SA, Badger MR, Andrews TJ, von Caemmerer S. 2000. Photosynthetic electron sinks in transgenic tobacco with reduced amounts of Rubisco: little evidence for significant Mehler reaction. *Journal of Experimental Botany* **51,** 357–368.

Sage RF, Christin P-A, Edwards EJ. 2011. The C$_4$ plant lineages of planet Earth. *Journal of Experimental Botany* **62,** 3155–3169.

Sage RF, Sage TL, Kocacinar F. 2012. Photorespiration and the evolution of C$_4$ photosynthesis. *Annual Review of Plant Biology* **63,** 19–47.

Sheen J-Y, Bogorad L. 1985. Differential expression of the ribulose bisphosphate carboxylase large subunit gene in bundle sheath and mesophyll cells of developing maize leaves is influenced by light. *Plant Physiology* **79,** 1072–1076.

Sheen J. 1999. C$_4$ gene expression. *Annual Review of Plant Physiology and Plant Molecular Biology* **50,** 187–217.

Soros CL, Dengler NG. 2001. Ontogenetic derivation and cell differentiation in photosynthetic tissues of C$_3$ and C$_4$ Cyperaceae. *American Journal of Botany* **88,** 992–1005.

Stockhaus J, Schlue U, Koczor M, Chitty JA, Taylor WC, Westhoff P. 1997. The promoter of the gene encoding the C$_4$ form of phosphoenolpyruvate carboxylase directs mesophyll-specific expression in transgenic C$_4$ *Flaveria* spp. *The Plant Cell* **9,** 479–489.

Vogan PJ, Frohlich MW, Sage RF. 2007. The functional significance of C$_3$–C$_4$ intermediate traits in *Heliotropium* L. (Boraginaceae): gas exchange perspectives. *Plant, Cell and Environment* **30,** 1337–1345.

von Caemmerer S. 1989. A model of photosynthetic CO$_2$ assimilation and carbon-isotope discrimination in leaves of certain C$_3$–C$_4$ intermediates. *Planta* **178,** 463–474.

von Caemmerer S. 2000. *Biochemical models of leaf photosynthesis*. Collingwood, Australia: CSIRO Publishing.

von Caemmerer S, Furbank RT. 2003. The C$_4$ pathway: an efficient CO$_2$ pump. *Photosynthesis Research* **77,** 191–207.

Voznesenskaya EV, Edwards GE, Kiirats O, Artyusheva EG, Franceschi VR. 2003a. Development of biochemical specialization and organelle partitioning in the single celled C$_4$ system in leaves of *Borszczowia aralocaspica* (Chenopodiaceae). *American Journal of Botany* **90,** 1669–1680.

Voznesenskaya EV, Franceschi VR, Artyusheva EG, Black CC Jr, Pyankov VI, Edwards GE. 2003b. Development of the C$_4$ photosynthetic apparatus in cotyledons and leaves of *Salsola richteri* (Chenopodiaceae). *International Journal of Plant Sciences* **164,** 471–487.

Voznesenskaya EV, Koteyeva NK, Akhani H, Roalson EH, Edwards GE. 2013. Structural and physiological analyses in Salsoleae (Chenopodiaceae) indicate multiple transitions among C$_3$, intermediate and C$_4$ photosynthesis. *Journal of Experimental Botany* **64,** 3583–3604.

Voznesenskaya E, Koteyeva NK, Chuong SDX, Ivanova AN, Barroca J, Craven L, Edwards GE. 2007. Physiological, anatomical and biochemical characterization of the type of photosynthesis in *Cleome* species (Cleomaceae). *Functional Plant Biology* **34,** 247–267.

Wakayama M, Ueno O, Ohnishi J. 2003. Photosynthetic enzyme accumulation during leaf development of *Arundinella hirta*, a C$_4$ grass having Kranz cells not associated with vascular tissues. *Plant and Cell Physiology* **44,** 1330–1340.

Wang J-L, Klessig DF, Berry JO. 1992. Regulation of C$_4$ gene expression in developing amaranth leaves. *The Plant Cell* **4,** 173–184.

Wang J-L, Turgeon R, Carr JP, Berry JO. 1993. Carbon sink-to-source transition is coordinated with establishment of cell-specific gene expression in a C$_4$ plant. *The Plant Cell* **5,** 289–296.

Wang P, Kelly S, Fouracre JP, Langdale JA. 2013. Genome-wide transcript analysis of early maize leaf development reveals gene cohorts associated with the differentiation of C$_4$ Kranz anatomy. *The Plant Journal* **75,** 656–670.